

CERN/PSCC/79 - 31

PSCC/P9

August 31st, 1979

P R O P O S A L

STUDY OF  $p\bar{p}$  AND  $p\bar{d}$  INTERACTIONS AT THRESHOLD IN  
GASEOUS  $H_2$  and  $D_2$  TARGETS

Mainz - München - TRIUMF - Zürich Collaboration

E.G. Auld<sup>1</sup>, D.A. Axen<sup>1</sup>, G.A. Beer<sup>2</sup>, M. Comyn<sup>1</sup>, M.K. Craddock<sup>1</sup>, W. Dahme<sup>3</sup>,  
K.L. Erdman<sup>4</sup>, U. Gastaldi<sup>5</sup>, G. Gräff<sup>5</sup>, H. Kalinowsky<sup>5</sup>, E. Kayser<sup>5</sup>,  
E. Klempt<sup>5</sup>, R. Landua<sup>5</sup>, Ch. Sabev<sup>6</sup>, R. Schulze<sup>5</sup>, P. Truöl<sup>7</sup>, J.B. Warren<sup>1</sup>,  
B.L. White<sup>1</sup>, E. Winkelmann<sup>7</sup>, R.W. Wodrich<sup>5</sup>, C. Zupancic<sup>3</sup>.

Spokesman : E. Klempt

Contactman : U. Gastaldi

- 1) University of British Columbia, Vancouver, Canada.
- 2) University of Victoria, Canada.
- 3) University of München, West Germany.
- 4) TRIUMF, Vancouver, Canada.
- 5) University of Mainz, West Germany.
- 6) CERN Visitor, Geneva, Switzerland
- 7) University of Zürich, Switzerland.

CONTENTS

pg.

Physics	2
Experimental apparatus	6
Count rate estimates	10
Requests	11
References	12
Tables	15
Figures	23

## I. PHYSICS

We propose to study the antiproton-proton and antiproton-deuteron strong interactions at threshold by stopping antiprotons in a gaseous target.

Investigations of the antiproton-nucleon strong interaction at threshold started long time ago with bubble chamber experiments and continued with counter experiments making use of liquid  $H_2(D_2)$  targets. In bubble chamber experiments (1, 11) branching ratios for annihilation at rest in liquid into pionic and kaonic final states were measured (see e.g. tables 1 - 4),  $\bar{p}N$  coupling to mesonic resonances was studied, evidence of dominant annihilation from initial atomic S-wave orbitals was produced and evidence for  $\bar{p}n$  quasinuclear/baryonium bound states was reported. Counter experiments concentrated on rare annihilation channels (e.g.  $\bar{p}p \rightarrow e^+ e^-$  (12)) and on annihilation channels with many neutrals (e.g.  $\bar{p}p \rightarrow \pi^0 \pi^0$  (13, 14),  $\bar{p}p \rightarrow \gamma + \text{anything}$  (15) in the final state). Comparison of  $\bar{p}p$  annihilation branching ratios into  $\pi^0 \pi^0$  and into  $\pi^+ \pi^-$  pointed to an important P wave annihilation component in the  $\bar{p}p \rightarrow 2\pi$  channel and has cast doubt on the usual assumption of dominant S wave annihilation in liquid hydrogen supported by bubble chamber data (16). Evidence has been reported of detection of direct  $\gamma$  transitions from initial  $\bar{p}p$  atomic states to narrow states below threshold (quasinuclear bound states or baryonium states). Several counter experiments at present on the floor at CERN and at Brookhaven search for baryonium states produced in reactions at threshold of antiprotons stopped in liquid targets. All these experiment use liquid targets to get a viable rate of stopped antiprotons.

Antiproton nucleon strong interaction at threshold (annihilation, elastic scattering, off shell charge exchange...) are generally assumed to occur in atomic orbitals of the antiprotonic atom that forms when an antiproton is stopped inside the target. Direct evidence of formation of antiprotonic hydrogen and deuterium atoms has indeed been established by detecting the characteristic radiative transitions to the 2P atomic

energy level in a recent experiment (17,18) where, for the first time, use was made of a gas target at room temperature.

In experimental studies of  $\bar{p}p$  and  $\bar{p}d$  strong interaction at threshold performed so far the quantum numbers of the initial atomic state of  $\bar{p}p$  and  $\bar{p}n$  annihilation are not measured. Inferences on the angular momentum of the initial atomic state was possible only for special annihilation channels for which the initial state is restricted by selection rules (see e.g. table 5 (19)). Furthermore, poor solid angle, energy resolution and detection efficiency for detection of neutral particles limit the information on the final state in annihilation reactions, and no direct measurements of the  $\bar{p}p$  and  $\bar{p}d$  S-wave scattering length and P-wave scattering volume are available.

We are therefore at present still far from a complete phenomenological picture of the  $\bar{N}N$  interaction at rest. While the strong interaction is, of course, governed by the unknown underlying dynamics, the phenomenological picture also depends on details of the atomic cascade and thus on the target density. Indeed the balance between S and P atomic wave annihilation depends on the Stark mixing of atomic orbitals occurring in collisions of the antiprotonic atom with the molecules of the target medium (20), and the rate of these collisions depends obviously on the target density.

At threshold the strong  $\bar{N}N$  interaction manifests itself by shifting and broadening the Coulomb levels of  $\bar{p}p$  and  $\bar{p}d$  atoms, by causing annihilation and by determining the annihilation pattern (branching ratios of annihilation final states for any initial atomic state depopulated by annihilation). Shift  $\Delta E$  and broadening  $\Gamma$  of the  $\bar{p}p$  and  $\bar{p}d$  Coulomb atomic levels are expected to depend strongly on the total spin state (hyperfine splitting due to the spin dependence of  $\bar{N}N$  forces) and on the existence in the proximity of the threshold of resonances and quasinuclear  $\bar{p}N$  bound states in the same spin state. These effects are, of course, more pronounced in atomic states of low principal quantum number  $n$ , because there, the overlap of the antiproton wave function with the proton (deuteron) is higher. Shifts and broadening of the 1S levels and broadening of

the  $2p$  levels of  $\bar{p}p(\bar{p}d)$  atoms look measurable with present detection techniques (see table 6 and 7 and ref.(21-35) for the  $\bar{p}p$  case) if one manages to populate appreciably the  $1S$  and  $2P$  levels and to detect the feeding X-ray radiative transitions (K and L lines, QED transition energies are given in table 8). Moreover, by detecting X-ray transitions in coincidence with annihilation products, it would be possible to separate individually P wave and S wave annihilation events and even, depending on the hyperfine splitting of the  $1S$  levels and on the resolution of the X-ray detector, to separate S wave annihilation events of different spin states.

We propose an experiment to measure in a gaseous target at ambient temperature and pressure  $p \leq 4$  atm. :

- a) energies, widths and yields of K and L X-ray transition in  $\bar{p}p$  and  $\bar{p}d$  antiprotonic atoms;
- b) ratios of  $\bar{p}p$  and  $\bar{p}d$  annihilations with charged particles in the final state (annihilation prongs multiplicity distributions).

The main aim of this experiment is to detect radiative transitions to the  $n = 1$  levels of  $\bar{p}p$  and  $\bar{p}d$  atoms (K-lines) and to obtain the low energy  $\bar{p}p(\bar{p}d)$  complexe S-wave scattering a from the measurement of shift and width of the levels :

$$\Delta E + i \frac{\Gamma}{2} = \frac{-1}{2m} |\psi_{1S}(0)|^2 a$$

We will try to resolve the ground state hyperfine structure and to measure  $\Delta E$  and  $\Gamma$  of each hyperfine sublevel, by selecting K X-rays in coincidence with specific annihilation channels allowed only from one given initial spin state (e.g.  $\bar{p}p$  K X-rays detected in coincidence with annihilation into neutral pions only must have populated the singlet  $1^1S_0$  state).

The  $\bar{N}N$  scattering length in a given spin and isospin channel is influenced by the existence of quasinuclear or baryonium states near threshold in the same channel. Determination of scattering lengths in the

$\bar{p}p$  and  $\bar{p}d$  channels may therefore help to assign quantum numbers to baryonium states established in independent experiments or point to the existence of new baryonium states.

At present only upper limits on the yield of the K lines are available. These limits depend strongly on the assumption made on the width of the K lines and range from some  $10^{-4}$  in liquid  $H_2$  (36,37) to  $10^{-2}$  in  $H_2$  and  $D_2$  gas at 4 atm (17, 18). We plan to reduce substantially the X-ray background in the proposal experiment, so to be sensitive to a K lines yield below  $10^{-3}$  in gas at 4 atm.

We intend to measure the annihilation width of the 2P level by comparing the intensity of the  $K_{\alpha}$  X-ray line (2P-1S transitions) to the intensity of the L lines that populate the 2P level. In the previous experiment S 142 performed at CERN with a gas target at 4 atm the yield of L X-rays was measured to be ~5%, and a lower limit on the annihilation width of the 2p level was obtained from the number of possible  $K_{\alpha}$  X-rays in the X-ray spectrum obtained requiring in coincidence a X-ray in the L X-ray energy region (17, 18). This coincidence technique is extremely powerful in reducing background. The X-ray detector designed for the proposed experiment will optimize the detection efficiency and maximize the background rejection for X-rays in the L energy region so to allow systematic use of the L X-ray coincidence technique.

We intend to measure the multiplicity distributions of annihilation reactions with charged particles in the final state and to compare the results with the existing ones in liquid targets. Furthermore we will be able to measure these distributions in coincidence with L and K X-rays. If the distributions of charged particle multiplicities for annihilations from P (L X-ray in coincidence) and S (K X-ray in coincidence) will turn out to differ significantly, this will provide an easy method to determine the ratio between S and P wave annihilation.

The experimental approach of the proposed experiment (choice of gaseous target and of a  $4\pi$  X-ray detector) and the design of the apparatus are

based on experience made during experiment S 142.

The apparatus is designed with the aim of reducing by more than one order of magnitude the physical X-ray background produced by the  $\bar{p}$  annihilation prongs.

At the end of the proposed experiment, to be carried out at a conventional low energy  $\bar{p}$  beam (K<sub>23</sub> e.g.), the apparatus would be well suited and tested for a first generation experiment at LEAR. A letter of intent for use of the proposed experimental apparatus at LEAR to search for specific  $\bar{p}p$  and  $\bar{p}d$  annihilation channels in coincidence with atomic X-rays will be submitted at a convenient time.

## II EXPERIMENTAL APPARATUS

The design of the present apparatus profits of the experience made by part of our collaboration with a previous one used in experiment S142 at CERN in 1976-78, and foresees substantial improvements :

- a) in the technique of detection of the X-rays;
- b) in the identification of the  $\bar{p}$  annihilation prongs;
- c) in the definition of the  $\bar{p}$ -STOP trigger (that indicates that an incoming antiproton stopped in the useful volume of the gas target).

The apparatus (fig.1) will consist of :

- i) a  $\bar{p}$  beam defining telescope
- ii) a system of plastic scintillators to make a fast selection of antiprotons likely to stop in the gas target
- iii) a gaseous H<sub>2</sub>(D<sub>2</sub>) target
- iv) an X-ray detector surrounding the gas target
- v) a concentric system of cylindrical wire chambers to detect the  $\bar{p}$  annihilation prongs
- vi) a set of plastic scintillators to provide a fast timing of  $\bar{p}$  annihilations.

All the components of the apparatus are contained in a cylindrical

pressure vessel ( $\phi = 80$  cm, length 120 cm) standing 5 atm pressure, apart the beam telescope and the annihilation plastic scintillators surrounding the vessel. The target gas is contained in a cylindrical volume ( $\phi = 30$ cm) in the centre of the vessel. The surrounding region is filled with a proportional gas mixture at the same pressure of the target gas and contains the X-ray detector (XDC) and two concentric arrays of drift chambers (IDC and EDC) used to detect the annihilation prongs. The separation between the two regions of the vessel is ensured in correspondence of the X-ray detector by a thin aluminized mylar tube (6 or 12  $\mu$ m thick) which has good transission for  $\bar{p}p$  ( $\bar{p}d$ ) X-rays down to energies  $\sim 1$ KeV.

### $\bar{p}$ Stop trigger

Beam particles entering the STOP volume are identified as antiprotons by TOF and  $dE/dx$  in a beam telescope including plastic scintillators outside the pressure vessel and T1 and T2. Antiprotons likely to stop in the STOP volume are at the end of their range and can be identified by their high energy loss in T2. Antiprotons with high energy loss in T2 that do not stop in the gas of the STOP volume, stop in T4 or stop in or traverse the XDC. In any case they deposit in T4 or in XDC much more energy than pions from  $\bar{p}$  annihilation can do. We will therefore use as  $\bar{p}$ -STOP trigger the signal (BEAM TELESCOPE,  $T2_H$ ,  $\overline{T3}$ ,  $\overline{T4_H}$ ,  $\overline{XDC_H}$ ); the subscript H indicates use of high discrimination thresholds excluding firing on pions from  $\bar{p}$  annihilation.

We intend to use in this experiment the same scintillators used as T counters in the previous experiment S142, with some little modifications.

Use of the X-ray detector as veto counter for antiprotons was tested succesfully at the end of experiment S142.

The peak of the  $\bar{p}$  stop distribution will be placed in the center of the STOP volume by adjusting the thickness of a thin grafite moderator outside the pressure vessel. Most of the beam energy degradation will be done by a copper moderator located inside the pressure vessel against T2.



### X-ray detection

The X-ray detector (XDC) will be a cylindrical X-ray drift chamber (38).

The cylindrical XDC will be a one-gap multicell gas proportional and drift chamber. The chamber will consist of 128 drift cells corresponding to 128 sense wires stretched parallel to the target and chamber frame common axis and kept at ground potential (fig.2). The sense wires ( $\phi=20\mu\text{m}$  stainless steel) will be separated by intermediate wires stretched at the same radius ( $\phi = 100\mu\text{m}$  copper beryllium) and biased at a negative potential. Primary ionization electrons produced in a cell by X-ray absorption or by ionizing particles will drift radially towards the sense wire under the action of a radial electric field obtained by biasing at a high negative potential the aluminized mylar membrane that acts as a cathode surface for all 128 cells. The mylar membrane will be kept in a stable position and a good smooth cylindrical shape by applying an overpressure of  $\sim 1$  torr on the target gas side. A stability of the overpressure of better than 0.1 torr at all working pressures will be obtained using the gas regulation system of past experiment S142. This condition is sufficient to avoid gain and drift velocity changes due to unwanted movements of the membrane. A  $6\mu\text{m}$  thick membrane has a transparency  $T > 40\%$  for normal incident X-rays with energy exceeding 1.7 KeV (all  $\bar{p}p$  L lines satisfy this condition) and satisfies reliability requests (one  $6\mu\text{m}$  membrane has operated for longer than 1 year without damage in experiment S 142).

The 128 sense wires will be grouped in 64 pairs (U pairs) connected at the downstream end of the chamber. Each sense wire will be connected to a charge preamplifier installed on the upstream frame of the XDC and immersed in the proportional gas mixture.

X-ray identification and charge division technique will be applied on each U pair. Discrimination against background from  $\bar{p}$  annihilation prongs will be performed:

- 1) by pulse-shape analysis following the technique used in exp.S142

- ( 39 ) that is based on the fact that pulses due to X-rays are short because of the strongly localized energy deposition;
- 2) by discarding X-ray candidate pulses located in XDC cells for which adjacent XDC cells and/or IDC cells have fired.

Energy and drift time calibration of the XDC will be performed following the techniques indicates in ref. 39 using tagged X-ray sources ( $Mn^{54}$  and beam induced Ar fluorescence). Charge division calibration could be performed by rotating the vessel by  $90^\circ$  in vertical position, and shooting into the middle of the chamber cells minimum ionizing pions with an horizontal bending magnet otherwise used to share the beam line with a second user.

The XDC will provide the following information :

- a) energy of the X-rays (from amplitude of linear pulse obtained by adding the signals of the amplifiers connected to the U pair of sense wires; expected energy resolution is  $< 20\%$  FW HM at 5.5 KeV),
- b) complete three dimensional localization of X-ray absorption points ( $\phi$  from U cell number and charge division, that defines which of the two sense wires of a given U fired;  $z$  from charge division;  $r$  from measurement of the drift length in the radial direction of the primary electrons produced when an X-ray is absorbed in one cell.

Information b) can supplement information a) quite efficiently as the absorption length of low energy X-rays (for which the amplitude resolution is poor as  $\frac{\Delta E}{E} \propto \frac{1}{E}$ ) depends strongly on the X-ray energy and this is reflected in the drift time distribution. As an example consider that the  $L_{\alpha}$  pp line (1.7 KeV) has a mean free path in Ar at 1 atm of  $\sim 7$ mm ( $\sim 2$ mm at 4 atm) and the  $L_{\infty}$  pp line (3.1 KeV) has a mean free path of  $\sim 30$  mm in 1 atm Ar ( $\sim 8$ mm at 4 atm) and an accuracy of 1mm in drift distance measurement can be obtained without major effort.

### Annihilation vertex and prongs multiplicity

The Internal Drift Chamber (IDC) and External Drift Chamber (EDC) will be used to detect the  $\bar{p}$  annihilation prongs and reconstruct the annihilation vertex. The EDC will consist of two staggered layers of sense and field wires to allow to resolve the left-right ambiguity.

The IDC and EDC will be similar in conception to the chamber described in ref. 39 . The chambers will consist of 64 cells and 128 cells respectively corresponding to the sense wires ( $\phi = 20 \mu\text{m}$  stainless steel) biased at a positive high voltage, alternating with field wires biased at negative voltage and sandwiched between cylindrical cathode surfaces defined by cathode wires set at ground potential. The sense wires will be grouped in U pairs as in the XDC. Charge division and drift time measurement will allow to determine the intercept of  $\bar{p}$  annihilation prongs with the cylindrical surfaces containing the sense wires. An accuracy  $\Delta z \sim \pm 1 \text{ cm}$  and  $\Delta(R\phi) \approx \pm 1 \text{ mm}$  are aimed at. Left right ambiguity in the IDC will be resolved by use of the XDC information.

Reconstruction of the annihilation vertex will ensure that  $\bar{p}$  annihilation did occur inside the target ( $\bar{p}p$  annihilation, e.g. and not annihilation in the mylar membrane or in the counter gas mixture). The efficiency of reconstruction of the annihilation vertex is limited by the solid angle coverage  $\Omega_{\text{EDC}}$  of the EDC ( $\Omega_{\text{EDC}} \geq 60\%$ ).

### III COUNT RATE ESTIMATES

In the  $K_{23}$  separated beam one can stop  $\sim 600$  antiprotons/burst in a liquid hydrogen target when  $\sim 3 \cdot 10^{12}$  protons hit the external production target. Hence we expect to stop  $\sim 1$  antiproton/burst in a gaseous hydrogen target at 1 atm. This value is supported by stop figures obtained in experiment S'142.

Within one PS period ( $\sim 4 \cdot 10^{18}$  protons on the production target) we

expect the following count rates :

	H <sub>2</sub>	D <sub>2</sub>
Stop in 4 atm gas	4.10 <sup>6</sup>	4.10 <sup>6</sup>
L X-rays emitted	2.5.10 <sup>5</sup>	2.5.10 <sup>5</sup>
L X-rays detected	10 <sup>5</sup>	1.2.10 <sup>5</sup>
K X-rays emitted	5.10 <sup>3</sup>	250
L-K X-ray coincidences detected	1.6.10 <sup>3</sup>	100
L-K X-ray coincidences detected and no charged particle emitted	50	3

This estimate is made with the conservative assumption  $\Gamma_{\text{rad}} / \Gamma_{2P} = 0.02$  (0.001) for antiprotonic hydrogen (deuterium)

#### IV REQUESTS

We plan to have the apparatus operational in the second half of 1980.

We request three PS periods ( $\sim 10^{19}$  protons on the production target) for final in beam tests of the apparatus and for a measurement of the K X-ray energy of antiprotonic hydrogen and the hyperfine splitting of its ground state.

We need access to the experimental area for installation of the experiment at least one month before getting beam time. We would like to install the experiment on the floor at the end of the 1980 PS shut-down or during running in of the Antiproton Accumulator. We would like to share the beam with a second user by means of an horizontal bending magnet located at the end of the beam line.

In addition we would like to require CERN support for development and construction of the XDC counter, support for installation of the proposed experiment and access to the Electronics pool.

REFERENCES

- 1) M. Cresti et al., in Proc.Internat.Conf.Elementary Particles, Siena, 1963, 1, 263. Soc.Ital.di Fisica, Bologna.
- 2) R. Armenteros et al., Phys.Lett.17 (1965) 344 and ref. quoted therein
- 3) C. Baltay et al., Phys.Rev. 145 (1966) 1103 and ref. quoted therein.
- 4) A. Bettini et al., Nuove Cimento 47 (1967) 642 and ref. quoted therein.
- 5) L. Gray et al., Phys.Rev.Letters 26 (1971) 1491.
- 6) P. Frenkiel et al., Nuclear Physics B47 (1972) 61 and ref. quoted therein.
- 7) L. Gray et al., Phys.Rev.Letters 30 (1973) 1091.
- 8) R. Bizzarri et al., Nuclear Physics B69 (1974) 298.
- 9) R. Bizzarri et al., Nuclear Physics B69 (1974) 307.
- 10) T.E. Kalogeropoulos and G.S.Tsanakos, Phys.Rev.Letters 34 (1975) 1047.  
T.E. Kalogeropoulos and G.S.Tsanakos, in Proc. 3rd European Symposium on NN Interactions, Stockholm, 1976, (eds.G.Ekspong and S. Nilsson) (Pergamon Press, Oxford, 1977) p.29.
- 11) C.R. Sun et al., Phys.Rev. D14 (1976) 1188.
- 12) G. Bassompierre et al., Phys. Letters 64B (1976) 475.
- 13) S. Devons et al., Phys.Rev.Letters 27 (1971) 1614).

- 14) G. Bassompierre et al., in proc. 4th European Antiproton Symposium, Barr-Strasbourg, 1978, (Editions du CNRS, Paris, 1979) (edt. A. Friedman), Vol.1, p.139.
- 15) P. Pavlopoulos et al., Phys.Lett.72B (1978) 415.
- 16) For a review see R. Bizzarri, in Proc.Symposium on antinucleon-nucleon annihilations, Chexbres, (1972), (CERN 72-10, 1972, edt. L. Montanet) 161 and also ref. 8, 9 and 11.
- 17) E. Auld et al., Phys.Lett. 77B (1978) 454.
- 18) E. Auld et al., same proceedings as ref. (14), Vol.1 p.115
- 19) T.D. Lee and C.N. Yang, Nuovo Cimento 3 (1956) 749.
- 20) T.B. Day, G.A. Snow and J. Sucher, Phys.Rev. 118(1960) 864.
- 21) B.R. Desai, Phys.Rev.119 (1960) 1385.
- 22) S. Caser and R. Omnès, Phys.Letters 39B (1972) 369.
- 23) O.D. Dalkarov and V.M. Samaoilov, JETP Letters 16 (1972) 249.
- 24) O.D. Dalkarov and B.O. Kerbikov, JETP Letters 21 (1975) 134.
- 25) V.E. Markushin, Preprint ITEP-164, Moscow (1976).
- 26) W.B. Kaufman and H. Pilkuhn, Phys.Letters 62B (1976) 165.
- 27) T.E.O. Ericson, Low-energy  $\bar{N}N$  interactions, Proc. 3rd European Symposium on Antinucleon-Nucleon Interactions, Stockholm, 1976 (eds. G. Espong and S. Nilsson) (Pergamon Press, Oxford, 1977), p.3.

- 28) T.E.O. Ericson and L. Hambro, *Ann.Phys.*107 (1977) 44.
- 29) O.D. Dalkarov, Preprint ITEP-135, Moscow (1977).
- 30) B. Kerbikov, Preprint CERN-TH 2394 (1977).
- 31) I.S. Shapino, *Phys.Reports* 35C (1978) 131.

---

- 32) A.E. Kudryavtsev, V.E. Markushin and I.S.Shapiro, *Sov.Phys. JETP* 47 (1978), 225.
- 33) W.B. Kaufmann and H. Pilkuhn, *Phys.Rev.*C17 (1978) 215.
- 34) W.B. Kaufmann, *Phys.Rev.* C19 (1979) 440
- 35) W.B. Kaufmann, Contributed paper to ICOHEPANS 8th, Vancouver, 1979.
- 36) R.E. Welsh, in proceedings of ICOHEPANS 7th, Zürich 1977, (Binkhäuser Verlag, Basel und Stuttgart,edt. M.P. Locher 1977) p.95.
- 37) M. Izycki et al., same proceedings of ref.(14), Vol.1 p.3
- 38) U. Gastaldi, *Nucl.Instrum.Methods* 157 (1978) 441.
- 39) U. Gastaldi et al., *Nuclear Instrum.Methods* 156 (1978) 257.

TABLE 1

Rates of  $p\bar{p}$  annihilations at rest in liquid hydrogen with charged prongs.

		$\Sigma$	$\bar{\Sigma}$
$p\bar{p} \rightarrow 0$ prongs			3.2
$p\bar{p} \rightarrow 2$ prongs	$\pi^+\pi^-$	0.32	42.6
	$\pi^+\pi^-\pi^0$	7.8	
	$\pi^+\pi^-\chi^0$	34.5	
$p\bar{p} \rightarrow 4$ prongs	$\pi^+\pi^+\pi^-\pi^-$	5.8	45.8
	$\pi^+\pi^+\pi^-\pi^-\pi^0$	19.7	
	$\pi^+\pi^+\pi^-\pi^-\chi^0$	21.3	
$p\bar{p} \rightarrow 6$ prongs	$\pi^+\pi^+\pi^+\pi^-\pi^-\pi^-$	1.9	3.8
	$\pi^+\pi^+\pi^+\pi^-\pi^-\pi^-\pi^0$	1.6	
	$\pi^+\pi^+\pi^+\pi^-\pi^-\pi^-\chi^0$	0.3	
$p\bar{p} \rightarrow$ non-pionic	$K\bar{K}$ etc.		4.6



TABLE 2

( from C. Baltay et al., Phys.Rev.Lett.15 (1965) 532 )

Rates for two-body annihilations of antiprotons at rest in liquid hydrogen.

Channel	Rate
$\pi^+\pi^-$	$(3.2 \pm 0.3) \times 10^{-3}$
$K^+K^-$	$(1.1 \pm 0.1) \times 10^{-2}$
$K^+K^-/\pi^+\pi^-$	$0.33 \pm 0.023$
$K_1^0K_1^0 + K_2^0K_2^0$	$(0.88 \pm 0.11) \times 10^{-3}$
$K_1^0K_2^0$	$(0.61 \pm 0.09) \times 10^{-3}$
$\pi^0\rho^{\pm}$	$(2.9 \pm 0.4) \times 10^{-2}$
$\pi^0\rho^0$	$(1.4 \pm 0.2) \times 10^{-2}$
$\rho^0\eta^0$	$(2.2 \pm 1.7) \times 10^{-3}$
$\rho^0\omega^0$	$(7.0 \pm 3.0) \times 10^{-3}$
$\rho^0\rho^0$	$(3.8 \pm 3.0) \times 10^{-3}$
$K^0K^{*0}$	$(1.2 \pm 0.2) \times 10^{-3}$
$K^{\pm}K^{\mp}$	$(0.92 \pm 0.16) \times 10^{-3}$
$K^{\pm}K^{\mp}$	$(1.3 \pm 0.5) \times 10^{-3}$
$K^0\bar{K}^{*0}$	$(2.9 \pm 0.5) \times 10^{-3}$

TABLE 3

( from R. Armenteros and B. French, in High Energy Physics, Vol.4, (1969), (Academic Press Inc., New-York, edt.E.H.S. Burhop ) p.286)  
 Contribution of pion states to  $\bar{p}p$  annihilation at rest in liquid hydrogen.

Final state	Resonant intermediate state	Percentage of all annihilations <sup>a</sup>	
		Cresti <i>et al.</i> (1963)	Baltay <i>et al.</i> (1966b)
multi $\pi^0$	—	—	$3.20 \pm 0.50$
$\pi^+ + \pi^-$	—	$0.33 \pm 0.04$	$0.32 \pm 0.03$
$\pi^+ + \pi^- + \pi^0$	—	$5.4 \pm 0.7$	$7.8 \pm 0.9$
$\pi^+ + \pi^- + m\pi^0 (m > 1)$	$\rho^0 \pi^0$	} $3.4 \pm 0.7$	$1.4 \pm 0.2$
	$\rho^\pm \pi^\mp$		$2.7 \pm 0.4$
$2\pi^+ + 2\pi^-$	—	$5.4 \pm 0.3$	$5.8 \pm 0.3$
$2\pi^0 + 2\pi^- + \pi^0$	$A_2^\pm \pi^\mp$	$\sim 1.8$	—
	$\rho^0 \pi^\pm \pi^\pm$	—	—
	$\rho^0 \pi^+ \pi^-$	$\sim 3.6$	$5.8 \pm 0.3$
	$\rho^0 \rho^0$	$< 0.6$	$0.4 \pm 0.3$
$3\pi^+ + 3\pi^-$	—	$22.6 \pm 0.7$	$18.7 \pm 0.9$
	$\omega \pi^+ \pi^-$	$5.2 \pm 0.3^b$	$3.8 \pm 0.4^b$
	$\omega \rho^0$	$0.6 \pm 0.3$	$0.7 \pm 0.3$
	$\rho^0 \pi^+ \pi^- \pi^0$	} $13.6 \pm 0.3$	$7.3 \pm 1.7$
	$\rho^\pm \pi^\mp \pi^+ \pi^-$		$6.4 \pm 1.8$
	$\eta \pi^+ \pi^-$	$1.9 \pm 0.6^c$	$1.2 \pm 0.3^c$
$\eta \rho^0$	—	$0.22 \pm 0.17^c$	
$2\pi^+ + 2\pi^- + m\pi^0 (m > 1)$	—	—	$21.3 \pm 1.1$
$3\pi^+ + 3\pi^-$	—	$1.7 \pm 0.2$	$1.9 \pm 0.2$
$3\pi^+ + 3\pi^- + \pi^0$	—	$1.7 \pm 0.2$	$1.6 \pm 0.3$
	$\omega + 2\pi^+ + 2\pi^-$	$1.3 \pm 0.3$	—
	$\eta + 2\pi^+ + 2\pi^-$	$0.6 \pm 0.2^c$	—
$3\pi^+ + 3\pi^- + m\pi^0 (m > 1)$	—	—	$0.3 \pm 0.1$

<sup>a</sup> Included in the percentage values for a given final state are those from resonant intermediate states. In addition, the rates for the production of  $\rho^0 \pi^+ \pi^-$ ,  $\omega \pi^+ \pi^-$ , and  $\eta^0 \pi^+ \pi^-$  include the contributions from events where the  $\pi^+ \pi^-$  were the decay products of a  $\rho^0$  meson.

<sup>b</sup> The following branching fraction has been used:  $(\omega \rightarrow \text{all})/(\omega \rightarrow \pi^+ \pi^- \pi^0) = 1.14$ .

<sup>c</sup> The following branching fraction has been used:  $(\eta \rightarrow \text{all})/(\eta \rightarrow \pi^+ \pi^- \pi^0) = 3.5$ .

TABLE 4

( from R. Armenteros and B. French, in High Energy Physics, Vol.4 (1969), (Academic Press Inc., New-York, edt.E.H.S. Burhop) p.383) :  
Rates of  $\bar{p}n$  annihilation at rest into pions in liquid deuterium.

Final state	Intermediate resonant state	Percentage of all annihilations <sup>a</sup>	
		Bettini <i>et al.</i> (1967)	Anninos <i>et al.</i> (1965)
$\pi^- + m\pi^0$ ( $m = 1, 2, \dots$ )	—	$16.4 \pm 0.5$	—
$\pi^- + \pi^0$	—	$\leq 0.7$	—
$2\pi^- + \pi^+ + m\pi^0$ ( $m = 0, 1, 2, \dots$ )	—	$59.7 \pm 1.2$	—
$2\pi^- + \pi^+$	—	$1.57 \pm 0.21$	—
	$\rho^0 + \pi^-$	(0.63)	—
	$f^0 + \pi^-$	(0.94)	—
$2\pi^- + \pi^+ + \pi^0$	—	$21.8 \pm 2.2$	—
	$\rho^+ + 2\pi^-$	—	( $0.9 \pm 0.4$ )
	$\rho^0 + \pi^- + \pi^0$	(8.7)	( $5.9 \pm 1.1$ )
	$\rho^- + \pi^+ + \pi^-$	—	( $3.9 \pm 0.8$ )
	$A_2^0 + \pi^0$	(3.3)	(0.5)
	$\omega^0 + \pi^-$	( $0.41 \pm 0.08$ )	( $0.38 \pm 0.15$ )
	$\eta^0 + \pi^-$	(0.25)	(0.2)
$3\pi^- + 2\pi^+ + m\pi^0$ ( $m = 0, 1, 2, \dots$ )	—	( $23.4 \pm 0.7$ )	—
$3\pi^- + 2\pi^+$	—	—	—
$3\pi^- + 2\pi^+ + \pi^0$	—	—	—
	$\omega + 2\pi^- + \pi^+$	( $12.0 \pm 3.0$ )	—
$4\pi^- + 3\pi^+ + m\pi^0$ ( $m = 0, 1, 2, \dots$ )	—	( $0.39 \pm 0.07$ )	—

<sup>a</sup> All resonant rates are included in those given for the corresponding final state. Resonant rates have been corrected to also take into account their decays into neutral particles.

TABLE 5

(19) Selection rules for  $\bar{p}p$  and  $\bar{p}n$  annihilation into pions only.

SELECTION RULES FOR  $\bar{p}p \rightarrow m\pi$  ( $m \leq 5$ )<sup>a</sup>

State	$J^P$	$C$	$I$	$G$	$2\pi^0$	$\pi^+\pi^-$	$3\pi^0$	$\pi^+\pi^-\pi^0$	$4\pi^0$	$\pi^+\pi^- + 2\pi^0$	$2\pi^+ + 2\pi^-$	$5\pi^0$	$\pi^+\pi^- + 3\pi^0$	$2\pi^+2\pi^-\pi^0$
$^1S_0$	$0^-$	+1	0	+1	X	X	Z	Z	—	—	—	Z	Z	Z
			1	-1	X	X	—	—	—	Z	Z	—	—	—
$^3S_1$	$1^-$	-1	0	-1	X	Z	X	—	X	Z	Z	X	—	—
			1	+1	X	—	X	Z	X	—	—	—	X	—
$^1P_1$	$1^+$	-1	0	-1	X	X	X	—	X	Z	Z	X	—	—
			1	+1	X	X	X	Z	X	—	—	—	X	Z
$^3P_0$	$0^+$	+1	0	+1	—	—	X	X	—	—	—	Z	Z	Z
			1	-1	Z	Z	X	X	Z	Z	Z	—	—	—
$^3P_1$	$1^+$	+1	0	+1	X	X	Z	Z	—	—	—	Z	Z	Z
			1	-1	X	X	—	—	Z	Z	Z	Z	—	—
$^3P_2$	$2^+$	+1	0	+1	—	—	Z	Z	—	—	—	Z	Z	Z
			1	-1	Z	Z	—	—	Z	Z	Z	Z	—	—

<sup>a</sup> From Lee and Yang (1956). X means strictly forbidden, i.e., by  $P$  and  $C$  conservation. Z means forbidden by  $G$  parity conservation.

SELECTION RULES FOR  $\bar{p}n \rightarrow m\pi$  ( $m \leq 5$ )<sup>a</sup>

State	$J^P$	$I$	$G$	$\pi^-\pi^0$	$2\pi^- + \pi^+$	$\pi^- + 2\pi^0$	$2\pi^- + \pi^+ + \pi^0$	$\pi^- + 3\pi^0$	$3\pi^- + 2\pi^+$	$2\pi^- + \pi^+ + 2\pi^0$	$\pi^- + 4\pi^0$
$^1S_0$	$0^-$	1	-1	X	—	—	—	—	—	—	—
$^3S_1$	$1^-$	1	+1	—	Z	Z	—	—	Z	Z	Z
$^1P_1$	$1^+$	1	+1	X	Z	Z	—	—	Z	Z	Z
$^3P_0$	$0^+$	1	-1	Z	X	X	Z	Z	—	—	—
$^3P_1$	$1^+$	1	-1	X	—	—	Z	Z	—	—	—
$^3P_2$	$2^+$	1	-1	Z	—	—	Z	Z	—	—	—

<sup>a</sup> From Lee and Yang (1956). X means strictly forbidden, i.e., by  $P$  or  $C$  conservation. Z means forbidden by  $G$  parity conservation.

TABLE 6

Expected shifts and widths ( $\Delta E + i \Gamma/2$ ) of the 1S levels of  $\bar{p}p$  atoms

$1^1S_0$	$1^3S_1$	Ref.
(0.53 + 0.15i)KeV	(0.6 + 0.15i)KeV	23
(0.59 + 0.36i)KeV	(0.96 + 0.31i)KeV	27
(0.43 + 0.050i)KeV	-	34
(0.50 + 0.68i)KeV	(0.75 + 0.50i)KeV	35

TABLE 7

Expected strong interaction width  $\Gamma_{2P}$  of the 2P level of  $\bar{p}p$  atoms and fractional  $K_{\alpha}$  x-ray yield from 2p state ( $\Gamma_{rad}$  is the 2P level radiative width,  $\Gamma_{rad} = 0.00037$  eV)

$\Gamma_{2P}$ (eV)	$\Gamma_{rad}/(\Gamma_{2P} + \Gamma_{rad})$	Ref.
0.009	0.04	21
0.037	0.01	33
0.013	0.03	34
0.022	0.02	35
0.00005	0.88	25
0.0005	0.42	25
0.0100	0.04	25
$\geq 0.004$	$\leq 0.1$	exp. S142 17,18

TABLE 8

QED transition energies in  $\bar{p}p$  and  $\bar{p}d$  atoms (eV)

$\bar{p}p$			$\bar{p}d$		
K series	L series	M series	K series	L series	M series
9.368	1 735	607	12491	2313	810
11.103	2 342	888	14804	3123	1184
11.710	2 623	1040	15989	3498	1388
11.992	2 776	1133	16192	3701	1511
.	.	.	.	.	.
.	.	.	.	.	.
12 491	3 123	1389	16655	4164	1851

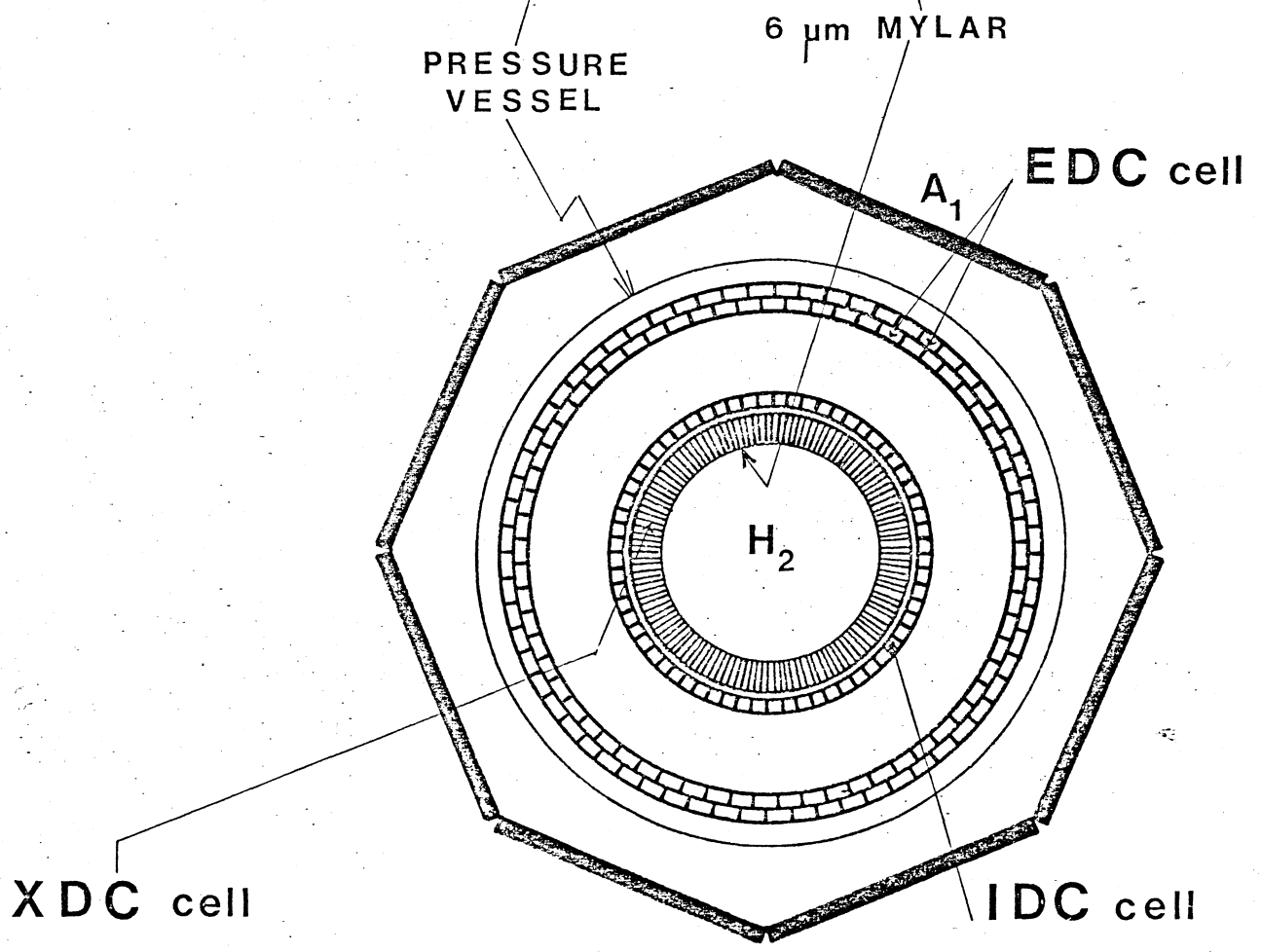
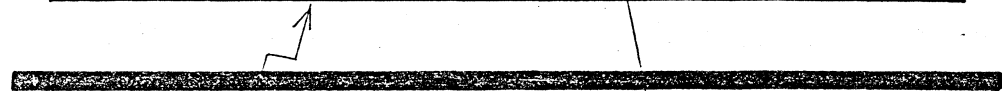
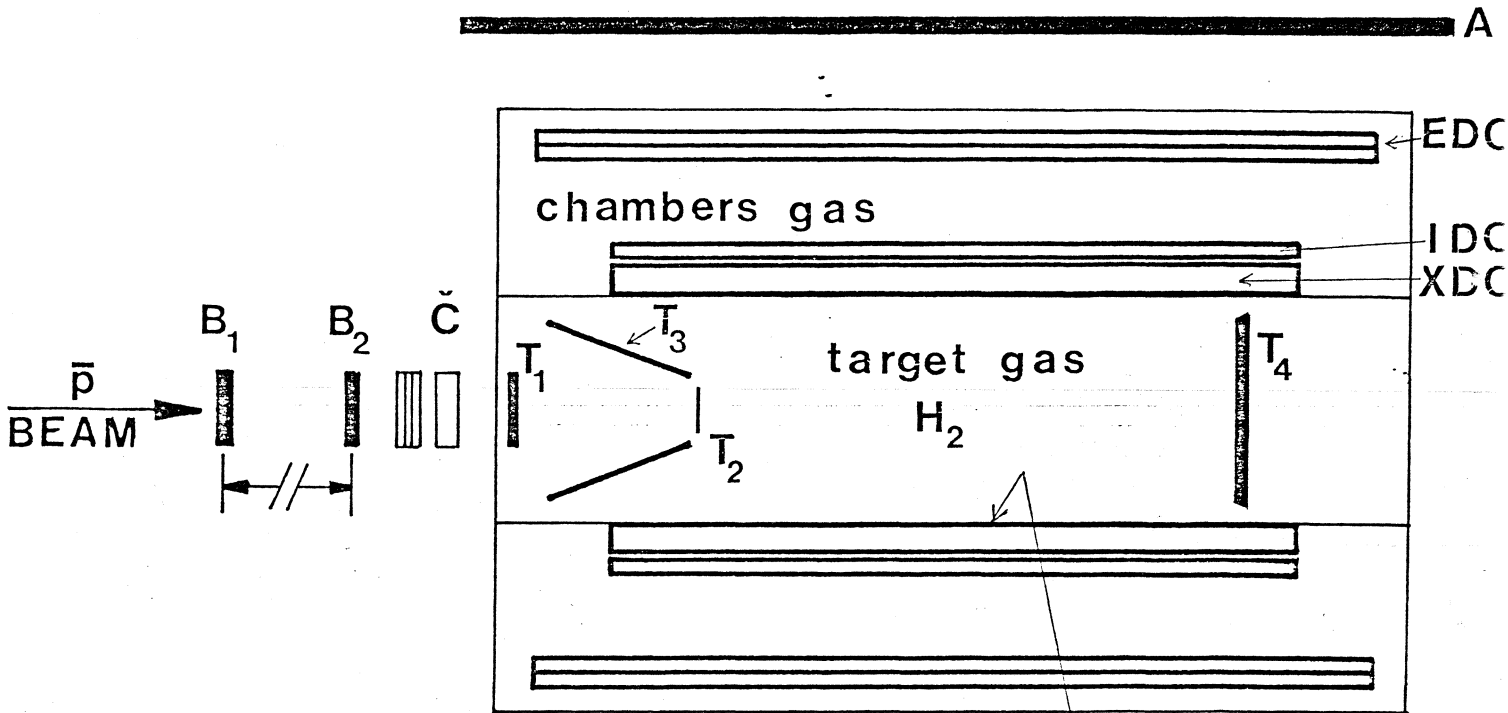


fig 1



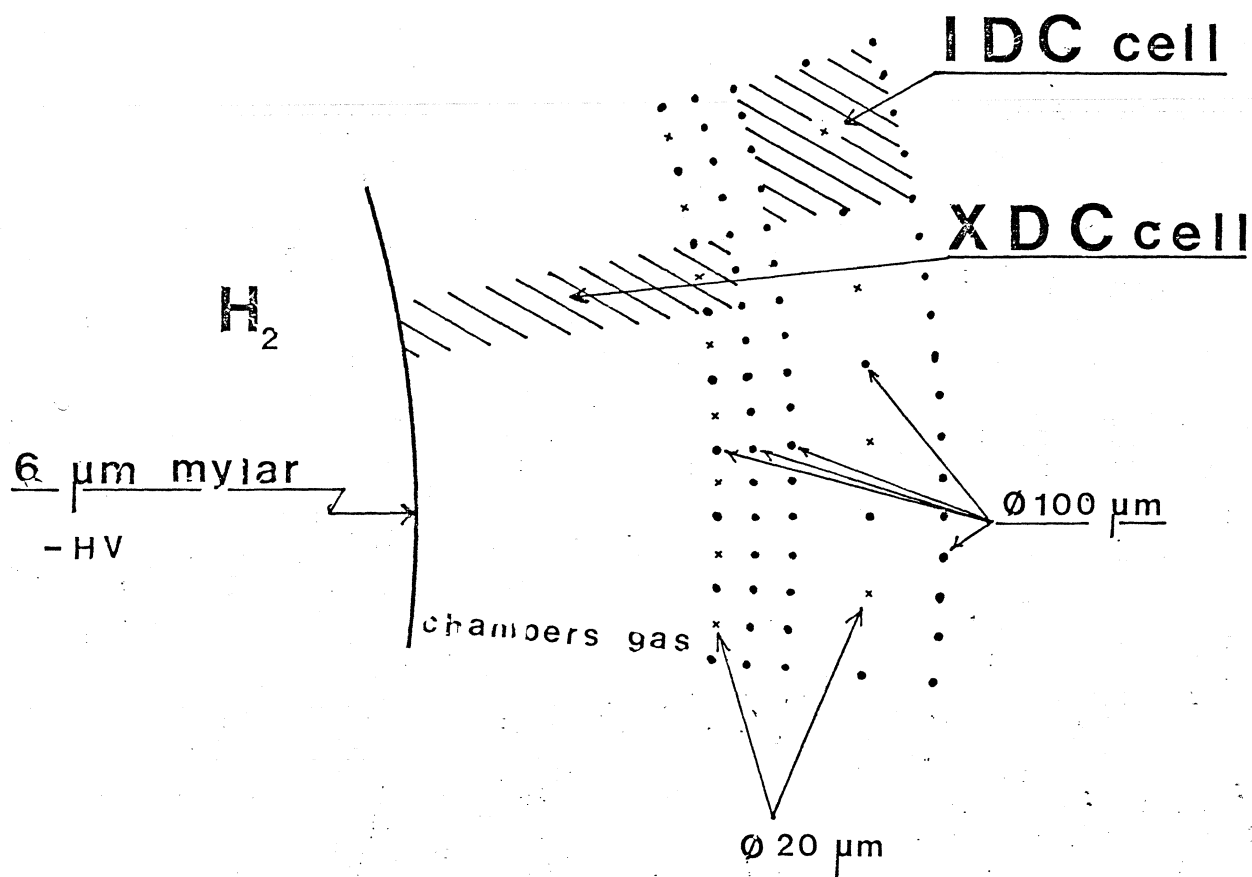


fig 2